

---

# AN EFFICIENT TRAINING PIPELINE FOR REASONING GRAPHICAL USER INTERFACE AGENTS

---

**Georgios Pantazopoulos\***  
 The Alan Turing Institute  
 Heriot-Watt University  
 gpantazopoulos@turing.ac.uk

**Eda B. Özyiğit**  
 The Alan Turing Institute  
 eozyigit@turing.ac.uk

## ABSTRACT

Visual grounding is the task of localising image regions from natural language queries and is critical for reasoning capable Graphical User Interface agents. Many existing methods rely on massive, noisy synthetic datasets. This work introduces an efficient training pipeline that combines model-based data filtering with parameter-efficient fine-tuning. From 4.8M synthetic examples, 12K clean and diverse instances are curated by first identifying challenging cases, removing misaligned and then selecting a diverse set of multimodal instances. On this data, a 3B-parameter Vision-Language Model is trained under three regimes: supervised fine-tuning, chain-of-thought- augmented fine-tuning, and reinforcement learning via Group Relative Policy Optimization. Models trained with the filtered data and lightweight training strategies match or surpass larger baselines on benchmarks such as ScreenSpot, Multimodal-Mind2Web, and AndroidControl. These results demonstrate that principled data curation and robust adaptation can rival large-scale training, enabling compact yet capable multimodal reasoning agents.<sup>1</sup>

## 1 Introduction

Visual grounding aims to link a natural language expression to its corresponding region in an image [1, 2, 3, 4, 5]. This capability is foundational for emerging Graphical User Interface (GUI) agents, as advances in Large Language Models (LLMs) and Vision-Language Models (VLMs) now enable these agents to execute natural-language instructions and control desktop, mobile, and web applications [6, 7, 8]. The core requirements are: multimodal perception to fuse visual and textual signals; and action execution to perform precise interface operations with mouse, keyboard, or touchscreen, commonly accompanied by lightweight planning and state tracking [9]. Reliable control begins with accurate grounding of instructions to specific GUI elements (e.g. buttons, icons) [10, 11, 12].

The main approach for developing such agents equipped with exceptional grounding capabilities is to fine-tune an existing VLM on a large-scale synthetic corpora [13, 14, 15, 16]. A typical pipeline first applies an off-the-shelf GUI element detector to produce candidate regions, then uses a VLM to generate referring expressions or step-level instructions tied to each region, yielding paired (screenshot, region, text) examples for supervision. This paradigm naturally leads to agents that perceive the environment exclusively through visual observations that match or surpass the performance of agents relying solely on text-based representations [13, 17, 18, 19]. However, naively fine-tuning requires large volumes of diverse data often exhibiting weak generalisation in complex and high-resolution professional settings. With the recent success of reinforcement learning (RL) as a post-training stage, concurrent efforts [20, 21, 21, 22] pivot to adopting RL by designing reward functions that promote more precise grounding and reasoning capabilities. Group Relative Policy Optimization (GRPO) [23], has recently emerged as one of the highly effective RL post-training regimes by replacing heavy value models with a simple rule-based reward system.

Furthermore, recent works [24, 25] challenge the claim that reasoning necessitates excessive amounts of training data demonstrating that reasoning can emerge with only a few clean and representative examples. On the other hand, employing synthetic pipelines for creating GUI training instances often result in noisy examples stemming from

---

\*Work done during the internship at The Alan Turing Institute.

<sup>1</sup>The code is available at <https://github.com/alan-turing-institute/gui-agent>

misaligned instruction-region pairs, low quality or repetitive instructions, and ambiguous regions often as a product of the detection algorithm.

Taken together, these observations call into question the necessity of high-volume synthetic instances for developing highly-capable GUI agents. In this work, we examine whether a highly-curated training seed can deliver comparable or superior performance, and explore the impact of different training regimes for building such agents. More specifically, we begin with a collection of high-volume synthetic training examples, and using a model-based filtering approach, we derive a clean, representative, and diverse set of examples for desktop, web, and mobile applications. Section 3 provides an overview of the stages of our filtering approach. From the initial pool of 4.8M examples, we select 12k demonstrations by determining challenging instances for the base VLM, and enforcing multimodal diversity, which yields about a compression rate of 400%. We provide the chain-of-thought (CoT) traces for the intended solution from a GUI agent and explore the impact of supervised fine-tuning and GRPO with simple sparse-based rewards. Our findings illustrate that our best-performing model matches or even surpasses the performance of similar and larger GUI agents both in terms of grounding capabilities as well as success rate in agentic evaluations.

The main contributions of this work are: (i) a detailed filtering method for curating misaligned synthetic data stemming from data generation pipelines using the same base-model as a critic for GUI training instances; (ii) a unified framework that applies model based filtering to web-based synthetic data and training state-of-the-art VLMs that is surprisingly effective for GUI agents; and (iii) a thorough evaluation of grounding and agent capabilities in GUI interfaces (desktop, mobile, and web). The results demonstrate that our agent achieves performance, at least comparable, and often substantially better, than the state-of-the-art agents.

## 2 Related Work

**GUI agents** LLMs and VLMs have significantly accelerated progress in the development of GUI agents. Early approaches relied on structured representations such as HTML or accessibility (a11y) trees [17, 18, 19] for grounding with labelled bounding boxes [26, 27]. However, text-based representations of these environments are often noisy and/or incomplete [13] while at the same time, encoding the structure of the interface raises significant computational overhead as opposed to its corresponding visual observation. [28] As a result, more recent work has shifted toward pixel-level, visually grounded agents that directly interpret screen-level observations, leveraging advances in visual encoders and multimodal reasoning to achieve robust performance in complex GUI environments [10, 13, 14, 15, 29, 30, 31]. Building upon these developments, frameworks such as UI-TARS [16] and AgentS2 [32] adopt modular or generalist-specialist architectures to improve reasoning, planning, and cross-platform generalisation [33, 34]. Nevertheless, the predominant reliance on supervised fine-tuning (SFT) [35] across these systems presents enduring challenges, including substantial data requirements, limited adaptability to unseen interfaces, and suboptimal scalability in dynamic GUI contexts [21, 22]. These limitations have motivated increasing interest in learning paradigms that can leverage interaction-based or self-supervised signals to achieve more flexible and data-efficient GUI understanding.

**Reinforcement Learning** Reinforcement learning (RL) has recently emerged as a promising alternative to SFT for training GUI agents, offering a mechanism to optimise model behaviour through interaction-based feedback rather than static supervision [36]. Rule-based reinforcement fine-tuning (RFT) paradigms have demonstrated impressive generalisation across reasoning, code generation, and multimodal perception tasks by employing verifiable reward signals to guide model adaptation [37, 38, 39]. Extending this paradigm to GUI environments, concurrent works such as UI-R1 [21] and GUI-R1 [20] have pioneered the integration of RFT for high-level interaction reasoning and low-level grounding, achieving improved action prediction accuracy even under limited data regimes. These approaches illustrate the potential of RL-based methods to enhance both the contextual understanding and decision-making efficiency of GUI agents. Furthermore, while the aforementioned works adopt rewards tailored exclusively to the performance of the agent, similar work [22] incorporates continuous reward formulations along with verifiable rewards that further guides the attention mechanisms of modern VLMs towards the target elements. Our work is aligned with aforementioned approaches, underscoring the promise of reinforcement-driven learning as a scalable and generalisable foundation for the next generation of intelligent GUI agents, capable of bridging perception, reasoning, and control within unified multimodal frameworks.

## 3 Method

### 3.1 Overview

This work follows the SeeAct-V framework [13], where an agent only uses screenshots as environmental observation. The original SeeAct-V has two stages: planning and grounding, both handled by a VLM. For grounding, SeeAct-V uses

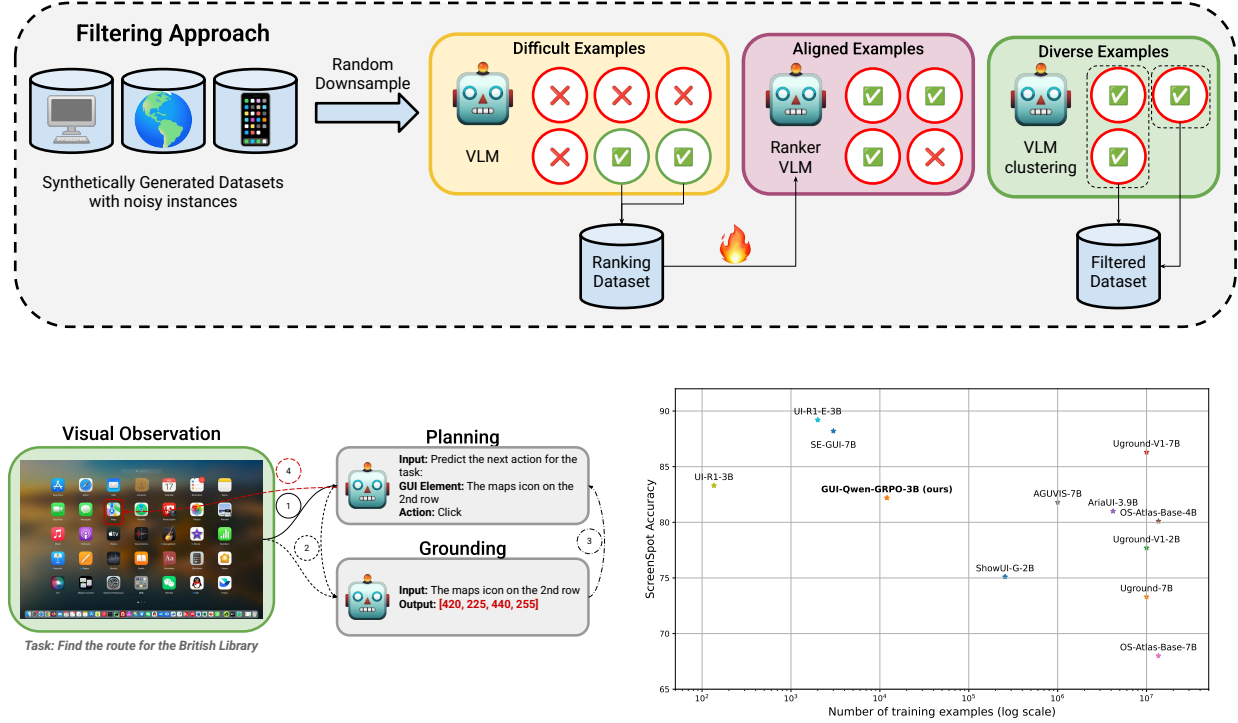


Figure 1: **(top)**: Overview of our filtering approach. We begin with a pool of noisy, GUI examples drawn from desktop, web, and mobile interfaces. A base VLM scores candidates, allowing us to partition the pool into easy and challenging cases. We train a ranking model on the easy subset to decide whether an instruction aligns with a candidate region in the interface. The ranker is then applied to the challenging subset to retain only aligned instances. We then cluster the embeddings from a single forward pass of the VLM and select a diverse set of challenging examples. **(bottom left)**: We integrate our grounding model into the SeeAct-V framework [13], which uses screenshots as the only environmental observations and performs pixel-operations via a planner VLM. **(bottom right)**: Grounding performance of ScreenSpot [10]. Our model significantly outperforms prior approaches relying on supervised fine-tuning over massive amounts of data and aligns with concurrent approaches combining RL+data filtering.

a separate model specialised for visual grounding that directly produces the coordinates on the current screen where the agent should act. As such a high-performing visual grounding model constitutes a necessary component for making SeeAct-V a compelling framework.

The development of GUI models is driven by synthetic data generation pipelines where GUI annotations are created either by (i) detecting elements in the interface via pre-trained detectors [40] or Set-of-Marks (SOM) [41] followed by a VLM that provides references for each detected element; or (ii) HTML parsing [28]. Ideally, the grounding model should generalise across platforms (e.g. web, desktop, and mobile) and handle diverse ways of referring to GUI elements. However, these pipelines often result in misaligned instances with limited variability. To address this issue, we propose a model-based filtering approach where the base VLM is used at different stages in Section 3.2. Finally, Section 3.3 outlines our model design choices and the training regimes via supervised fine-tuning, and eliciting reasoning via chain-of-thought and reinforcement learning.

### 3.2 Dataset & Filtering Pipeline

We start from a collection of existing open-source GUI grounding datasets including ShowUI-Desktop [15], and AriaUI [14] resulting in 4.8M grounding instances covering desktop, web, and mobile interfaces. Although these resources are valuable, their automatic pipelines often result in noisy annotations. To mitigate this, we employ a filtering scheme in order to select challenging, diverse, and clean examples as follows:

**Task-Difficulty** We utilise Qwen-2.5-VL-3B [42] in a zero-shot setting and generate bounding box predictions for each training example. If the prediction for an example is correct, we consider this example as easy otherwise the example is considered hard and include it in our dataset.

**Bounding-box Accuracy** Many training resources are created using an automatic setup, either by (i) creating SOM on GUI elements and then using a VLM to create references on each element; or (ii) using text-based representations by parsing the raw HTML or accessibility (ally) trees [17, 19]. However, due to noise in the collection process, the hard examples obtained from the previous step may not in fact have aligned instruction-bounding box pairs. To detect false-positive examples included in our dataset, we train a ranking model based on Qwen-2.5-VL-3B that determines whether an instruction-bounding box pair is valid. This ranking model is trained using the easy examples from the previous step (see Section 4.1 and Section B.1 for further information).

**Diverse Training Examples** An additional shortcoming of the existing resources is that the automatic data creation process results in repetitive examples. For instance, given a GUI representing a spreadsheet, many approaches relying in a combination SOM+VLM to create annotations, yields multiple examples that point to cell entities in the GUI often with limited language variation (e.g. “Click on Cell F42”). To select diverse and representative training examples, we employ one forward pass and obtain the last hidden state. We then cluster the hidden states using PCA and k-means then obtain the examples closer to each centroid.

**Post-Processing** Finally, we apply a post-processing filtering stage by using GPT-4o mini to further select examples where the instruction clearly points to the correct GUI element without any notion of ambiguity. At this stage, we also manually verified the correctness of our filtered examples.

We apply the above steps sequentially on the initial set of 4.8M examples. With this process, we curate a clean version with 12K examples which corresponds to roughly 0.25% of the original data. We also note that before applying the filtering, due to computational constraints, we also randomly downsampled the Aria dataset to 10% of its original size.

**Generating Chain-of-thought-traces** In addition to the filtered examples, we provide chain-of-thought traces derived from GPT-4o mini. Given the grounding instance, we highlighted the correct region and asked the model to provide a reasoning trace for deriving the solution (see Section A.2 for more details).

### 3.3 Model

**Model Architecture** In all of our experiments, we employ the instruction-tuned variant Qwen-2.5-VL-3B as our base model as it performs exceptionally well on grounding multimodal tasks and supports high-resolution image input both of which are necessary prerequisites for GUI agents. With regards to the image resolution, typical GUI screenshots are much larger than natural images leading to significant computational overhead. As a result, we resize images by preserving their aspect ratio to  $256 \times 28 \times 28$  minimum and  $1080 \times 28 \times 28$  maximum pixels, respectively.

Our goal is to explore various training regimes for efficiently developing GUI agents. For this purpose, we resort to parameter-efficient methods for training, with low-rank adaptation (LoRA) [43] being the most prominent approach. Within VLMs, the design choice of where to apply LoRA adapters depends on various factors. Applying adapters on the vision encoder and/or the visual connector can be particularly effective especially when the base model has not been exposed to the target visual domain. Conversely, language adapters can be effective when the base model is not familiar with the output text distribution. Finally, applying adapters to all components can be effective when the base model has not been significantly exposed to the target domain. In this work, following prior approaches [44], we explore the impact of LoRA adapters on the visual and the language backbone of a GUI-specific model. More specifically, we apply adapters on all linear modules and explore three variants: 1) adapters on the visual backbone and the connector; 2) adapters on the language backbone; and 3) adapters on all components of the VLM.

**Training Regime** With regards to the training objectives, we compare three standard methods: 1) Supervised fine-tuning (SFT), where the model directly predicts the candidate element in the interface; 2) Supervised fine-tuning with chain-of-thought traces (SFT+CoT) where the model first derives a plausible explanation and then provides the candidate element; and 3) Reinforcement Learning (RL) with verifiable rewards using GRPO [45]. From a practical standpoint, the textual format of a candidate element usually corresponds to 10-15 tokens. On the other hand, the context size usually is bloated with image tokens due to high-resolution demands and possibly text tokens that describe the task, output format, and the action space. As a result, the model can only spend a limited and finite amount of steps to reason over the context. Eliciting reasoning capabilities via prolonged generated output in the form of explanations can potentially alleviate this issue. However, it is not straightforward to compile reasoning traces that act as a good

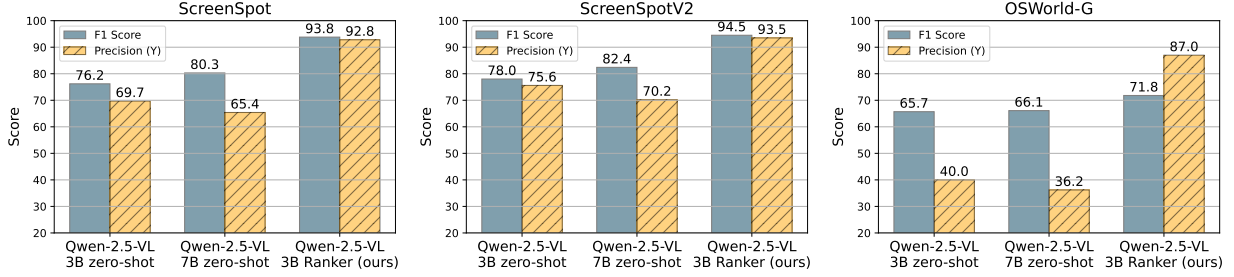


Figure 2: Performance of our ranking model against 3B/7B variants on ScreenSpot, ScreenSpotv2 and Osworld-G.

supervision signal for the model. For this reason, it is common to employ post-training RL by directly optimising performance via reward tailored to the downstream metric.

**Training Details** Throughout our experiments, we apply eight different LoRa configurations for the vision, language, and the joint model resulting in 24 different runs for each training regime. The best candidate for each training regime is determined by the grounding performance on GUI interfaces (Section 4.2), which is then used within the SeeAct-V framework (Section 4.3). For GRPO, we formulate our reward signal based on three scalar values: 1) *Format-based*, where the model receives +1 if the output follows the desired format else 0; 2) *Solution-based*, where the model receives +1 if the center of the predicted bounding box falls within the ground-truth region; and 3) *Length-based* as from preliminary experiments we observed that the model collapsed resulting in gibberish generations. For this purpose, we provide a +1 credit if the length of the output does not exceed 100 tokens else 0. The final reward is the sum of the above values without any additional scaling. Details regarding hyperparameters are presented in Section B.

## 4 Experiments

We begin with experiments regarding the quality of our ranker (Section 4.1) showcasing the effectiveness of our model on retrieving aligned instruction-bounding box instances. In Section 4.2, we evaluate the grounding capabilities of our model under two settings, human-generated instructions, as well as instructions generated from planners that highlight which tests for the end-to-end effectiveness of our model when integrated into the SeeAct-V framework. Finally, we integrate our agent within the See-Act-V framework, and conduct offline evaluations (Section 4.3), where our agent accepts instructions in web, mobile, and desktop applications and controls the interface of a GUI by predicting the low-level actions that satisfy a user instruction.

### 4.1 Ranker model

The ranking model is trained on instances where the base model correctly identifies the target element in the interface. More specifically, given an image-instruction/expression-bbox triplet the ranker predicts whether the instruction or the expression matches the element in the image indicated by the bounding box.

**Creating negative annotations** An important note here is to clarify how the negative image-instruction-bbox triplets are derived. In principle, we could randomly sample a candidate bounding box, though this approach yields easy negatives. Thus, during filtering, the ranking model will be heavily biased towards the positive class. For this reason, we include examples in the training set of the ranking model by grouping instances from the same image. Given an  $N$  annotations from the same image, we include this image in the training set if there are at least  $M$  correct predictions. Given that the AriaUI contains significantly more instances than ShowUI, we set  $M = 5$  for AriaUI and  $M = 1$  for ShowUI desktop, respectively. With this process, we create 15k instances corresponding to 130k positive image-instruction-bbox triplets.

For a given example during training, we create positive triplets by keeping the original annotations with 50% probability. For negative examples, we swap the bounding box in the triplet with a different candidate belonging to the same image. Note that in the cases where an image only contains a single annotation, this example is considered by default positive.

**Results** We provide intermediate evaluations that substantiate the effectiveness of our ranking model by converting ScreenSpot [10], Screenspotv2 [31] and Osworld-G [34], three popular GUI grounding benchmarks, that we converted into a binary classification, consistent with our training protocol. Similar to the training setup, we group instances from

Model	Params	ScreenSpot								ScreenSpotv2							
		Mobile		Desktop		Web		Average		Mobile		Desktop		Web		Average	
		Text	Icon	Text	Icon	Text	Icon	Micro	Macro	Text	Icon	Text	Icon	Text	Icon	Micro	Macro
Fuyu [46]	8B	41.0	1.3	33.0	3.6	33.9	4.4	-	19.5	-	-	-	-	-	-	-	-
CogAgent [29]	18B	67.0	24.0	74.2	20.0	70.4	28.6	49.6	47.4	-	-	-	-	-	-	-	-
SeeClick [10]	9.6B	78.0	52.0	72.2	30.0	55.7	32.5	55.8	53.4	78.4	50.7	70.1	29.3	55.2	32.5	55.1	52.7
OmniParser [40]	-	93.9	57.0	91.3	63.6	81.3	51.0	-	73.0	-	-	-	-	-	-	-	-
ShowUI-G [15]	2B	92.3	75.5	76.3	61.1	81.7	63.6	-	75.1	-	-	-	-	-	-	-	-
UGround-V1 [13]	2B	89.4	72.0	88.7	65.7	81.3	68.9	-	77.7	-	-	-	-	-	-	-	-
UGround-V1 [13]	7B	93.0	79.9	93.8	76.4	90.9	84.0	-	86.3	-	-	-	-	-	-	-	-
AriaUI [14]	3.9B	92.3	73.8	93.3	64.3	86.5	76.2	82.4	81.0	-	-	-	-	-	-	-	-
OS-Atlas-Base [31]	4B	85.7	58.5	72.2	45.7	82.6	63.1	70.1	68.0	87.2	59.7	72.7	46.4	85.9	63.0	69.2	71.9
OS-Atlas-Base [31]	7B	93.0	72.9	91.7	62.9	90.9	74.3	82.4	80.1	95.2	75.8	90.7	63.6	90.6	77.3	84.1	82.0
<i>SFT:</i>																	
GUI-Qwen (V)	3B	91.9	67.2	89.7	57.1	83.9	62.1	77.0	75.3	96.9	73.8	96.1	73.8	85.4	68.4	83.2	82.4
GUI-Qwen (L)	3B	93.4	71.2	95.4	62.1	86.1	70.4	81.2	79.8	89.1	66.5	88.9	59.5	84.6	60.8	76.5	74.9
GUI-Qwen (VL)	3B	95.6	69.9	93.3	67.9	85.7	68.4	81.4	80.1	96.9	79.1	95.6	69.0	85.4	71.7	84.0	82.9
<i>SFT+CoT:</i>																	
GUI-Qwen (V)	3B	86.4	63.8	86.6	57.9	83.9	59.2	74.4	73.0	89.1	66.5	88.9	59.5	84.6	60.8	76.5	74.9
GUI-Qwen (L)	3B	94.5	75.5	93.3	62.9	86.5	67.5	81.6	80.0	96.9	79.1	95.6	69.0	85.4	71.7	84.0	82.9
GUI-Qwen (VL)	3B	94.5	71.2	93.8	69.3	87.0	65.5	81.4	80.2	97.3	73.8	96.1	74.6	85.7	68.4	83.4	82.6
<i>GRPO</i>																	
GUI-Qwen (VL)	3B	<b>97.4</b>	<b>78.2</b>	<b>93.8</b>	<b>65.0</b>	<b>89.1</b>	<b>69.9</b>	<b>83.9</b>	<b>82.2</b>	<b>99.2</b>	<b>84.3</b>	<b>95.0</b>	<b>69.0</b>	<b>91.4</b>	<b>71.7</b>	<b>86.6</b>	<b>85.1</b>

Table 1: Grounding accuracy on ScreenSpot and ScreenSpotv2 (Standard Setting). (V/L/VL) denotes LoRA parameters on visual, language, or both backbones.

the same image. If an image contains  $n$  annotations, for each example  $i$ , we create  $n - 1$  negative examples by using the  $i$ -th instruction and all  $m$  ( $m \neq i$ ) bounding boxes from all remaining examples.

We note that in this type of evaluation 55.7% and 71.5% of the examples correspond to negative labels for ScreenSpot and Osgworld-G, respectively. For this reason, we primarily focus on the overall F1-score and the precision of the positive class as we are interested in measures that quantify the correctness of the filtering approach for true-positive instances. As shown in Figure 2, our ranking model outperforms the 3B/7B zero-shot variants, demonstrating its effectiveness within our data filtering pipeline. However, we also report overall performance metrics including F1-score, accuracy, precision, and recall, along with class-specific metrics provided in in Section B.1.

Finally, we note two important caveats regarding these results. First, the benchmarks contain clean, human-generated annotations, which likely yield an optimistic estimate of model performance on the noisy, synthetic data prevalent in training resources. Second, while these benchmarks serve as the best available proxy for evaluating quality-filtering models on GUI instances, the performance gap between clean benchmark and noisy training data remains uncertain. Despite these limitations, the results provide evidence for the viability of our ranking-based filtering approach.

## 4.2 GUI Visual Grounding

We begin by evaluating the grounding performance of our model on ScreenSpot [10] and ScreenSpotv2 [31], which are specifically designed for visual grounding on GUIs. Both benchmarks consist of 1,272 single-step instructions and the corresponding bounding boxes of the target elements across mobile (e.g. iOS and Android), desktop (e.g. macOS and Windows), and web environments. The target elements encompass diverse GUI component types, including text-based elements, icons (e.g. trash can icons), and widgets (e.g. to-do lists).

Furthermore, following prior work [13], we focus on two settings: 1) Standard Setting, where the instructions are written by human annotations targeting a functional description of the element (e.g. simply “close” to refer to the “X” button that closes a window); and 2) Agent Setting, where the grounding model accepts instructions from a planning model that focus not only functional descriptions but also visual and positional information. To isolate the effects of instruction quality from grounding capability, we employ the instructions generated by Uground [13]. We primarily compare our approach against several state-of-the-art models of similar size on ScreenSpot and ScreenSpotv2.

**Results** We report the grounding accuracy in the Standard and Agent setting in Table 1 and Table 2, respectively. Among the SFT variants, GUI-Qwen (VL) with LoRA parameters on both visual and language backbones performs on

Model	Params	Mobile		Desktop		Web		Average	
		Text	Icon	Text	Icon	Text	Icon	Micro	Macro
SeeClick [10]	9.6B	81.0	59.8	69.6	33.6	43.9	26.2	-	52.3
UGround-V1 [13]	2B	94.1	77.7	92.8	63.6	90.0	70.9	-	81.5
UGround-V1 [13]	7B	94.1	79.9	93.3	73.6	89.6	73.3	-	84.0
OS-Atlas-Base [31]	4B	94.1	73.8	77.8	47.1	86.5	65.5	76.8	74.1
OS-Atlas-Base [31]	7B	93.8	79.9	90.2	66.4	92.6	79.1	85.1	83.7
<i>SFT:</i>									
GUI-Qwen (V)	3B	92.3	66.4	90.2	57.9	83.5	61.7	77.0	75.3
GUI-Qwen (L)	3B	94.1	71.2	94.9	63.6	87.0	67.5	81.1	79.7
GUI-Qwen (VL)	3B	96.0	68.6	93.8	66.4	86.1	67.0	81.0	79.6
<i>SFT+CoT:</i>									
GUI-Qwen (V)	3B	87.6	65.5	86.6	58.6	85.2	61.7	75.6	74.2
GUI-Qwen (L)	3B	95.6	76.0	93.8	62.9	86.5	65.5	81.7	80.1
GUI-Qwen (VL)	3B	92.7	70.7	93.3	59.3	83.5	66.5	79.3	77.7
<i>GRPO</i>									
GUI-Qwen (VL)	3B	<b>97.1</b>	<b>77.7</b>	<b>93.8</b>	<b>63.6</b>	<b>88.7</b>	<b>70.4</b>	<b>83.6</b>	<b>81.9</b>

Table 2: Grounding accuracy on ScreenSpot (Agent Setting) with planner-generated referring expressions. (V/L/VL) denotes LoRA parameters on visual, language, or both backbones.

Model	Params	Planner	Cross-Task	Cross-Website	Cross-Domain	Macro Average
SeeClick [10]	9.6B	GPT-4o	32.1	33.1	33.5	32.9
UGround-V1 [13]	2B	GPT-4o	48.6	47.6	47.7	48.0
UGround-V1 [13]	7B	GPT-4o	50.7	48.1	48.5	49.1
<i>SFT:</i>						
GUI-Qwen (V)	3B	GPT-4o	48.2	46.5	45.5	46.7
GUI-Qwen (L)	3B	GPT-4o	49.3	47.1	46.3	47.6
GUI-Qwen (VL)	3B	GPT-4o	49.1	46.4	46.2	47.2
<i>SFT+CoT:</i>						
GUI-Qwen (V)	3B	GPT-4o	47.8	43.2	45.1	45.4
GUI-Qwen (L)	3B	GPT-4o	48.3	46.7	46.1	47.0
GUI-Qwen (VL)	3B	GPT-4o	47.7	46.2	46.5	46.8
<i>GRPO</i>						
GUI-Qwen (VL)	3B	GPT-4o	<b>48.9</b>	<b>47.2</b>	<b>48.2</b>	<b>48.1</b>

Table 3: Element accuracy on Multimodal-Mind2Web. (V/L/VL) denotes LoRA parameters on visual, language, or both backbones.

par or even surpass significantly larger models. Surprisingly, the integration of chain-of-thought reasoning shows mixed results depending on the backbone configuration. The combination of CoT+LoRA adapters on the vision backbone results in performance degradation compared to the SFT variant. However, GUI-Qwen (L) with SFT+CoT improves over the base SFT version, while GUI-Qwen (VL) with CoT maintains comparable performance to its SFT counterpart. We hypothesise that this partially stems from discrepancy between the format of the trace and the outputs of the base model. Most importantly, our GRPO-optimised GUI-Qwen (VL) model achieves state-of-the-art results across both benchmarks. Similar trends can be observed in the case of the Agent setting, with planner-based instructions.

### 4.3 Offline Agent Evaluation

In this section, we provide experiments regarding offline agent evaluation on MultimodalMind2Web, Android Control, and OmniAct encompassing web, mobile, and desktop applications following their standard evaluation protocol [28, 47, 48] described below. Importantly, we adopt the planner-generated instructions from Uground [13] in each benchmark to decouple the effect of the quality of the planner from the downstream performance. As such, our comparison is focused mostly with the Uground family of models.

**Web: MultimodalMind2Web** We use Multimodal-Mind2Web [28], which extends the original Mind2Web [19] benchmark using multimodal information for web tasks. These tasks are crowdsourced ensuring they represent genuine, practical needs that real users would encounter on these platforms. The test split consists of 1,013 tasks spanning over

100 different websites. Each task is defined by a high-level task instruction and a sequence of actions, with a screenshot of the webpage before each action, as the golden trajectory. We report element accuracy, i.e. accuracy of selecting the correct element, and omit operation scores because they are orthogonal to grounding comparisons.

Model	Params	Planner	High	Low
SeeClick [10]	9.6B	GPT-4o	41.8	52.8
UGround-V1 <sup>†</sup> [13]	2B	GPT-4o	50.0	65.0
UGround-V1 <sup>†</sup> [13]	7B	GPT-4o	49.8	66.2
<i>SFT:</i>				
GUI-Qwen (V)	3B	GPT-4o	34.2	60.0
GUI-Qwen (L)	3B	GPT-4o	34.8	62.6
GUI-Qwen (VL)	3B	GPT-4o	36.2	63.8
<i>SFT+CoT:</i>				
GUI-Qwen (V)	3B	GPT-4o	39.0	61.6
GUI-Qwen (L)	3B	GPT-4o	36.0	63.2
GUI-Qwen (VL)	3B	GPT-4o	37.4	62.0
<i>GRPO</i>				
GUI-Qwen (VL)	3B	GPT-4o	<b>44.0</b>	<b>66.0</b>

Table 4: Step accuracy (SA) on AndroidControl over 500 random actions from the test split. Models<sup>†</sup> are fine-tuned for this task.

Model	Params	Planner	Action Scores
SeeClick [10]	9.6B	GPT-4o	29.6
UGround-V1[13]	2B	GPT-4o	32.9
UGround-V1[13]	7B	GPT-4o	34.0
<i>SFT:</i>			
GUI-Qwen (V)	3B	GPT-4o	33.8
GUI-Qwen (L)	3B	GPT-4o	34.2
GUI-Qwen (VL)	3B	GPT-4o	34.0
<i>SFT+CoT:</i>			
GUI-Qwen (V)	3B	GPT-4o	33.2
GUI-Qwen (L)	3B	GPT-4o	<b>34.3</b>
GUI-Qwen (VL)	3B	GPT-4o	34.1
<i>GRPO</i>			
GUI-Qwen (VL)	3B	GPT-4o	33.8

Table 5: Action scores (AS) on OmniACT.

**Mobile: Android Control** For mobile applications, we use AndroidControl [47], a dataset with 15k tasks covering 833 apps. Each task is also densely annotated with low-level step by step instructions that correspond to an action. Following prior work [13, 47], we use a subset of 500 random steps from the original set and adopt two task settings: 1) high-level control where only the high-level intent is provided; and 2) low-level control, where both the high-level intent and the corresponding low-level instruction for each timestep are available. In both settings, we report the standard step-wise accuracy where a step is considered successful only if all the predicted actions, elements, and arguments (if applicable) are correct.

**Desktop: OmniAct** Finally, we evaluate our model on OmniACT [48], a collection of 9,802 tasks covering 38 desktop applications and 27 websites across different platforms. Each of these tasks requires the agent to provide a PyAutoGUI<sup>2</sup> script – a sequence of actions to complete the task on a single screenshot. We report the action score which measures how well a code snippet containing the correct action sequence can perform the task.

**Results** Results are presented in Table 3, Table 4, and Table 5 for Multimodal-Mind2Web, Android Control, and Omniact, respectively. Our GUI-Qwen models demonstrate competitive performance across all web, mobile, and desktop domains despite using only 3B parameters. On the Multimodal-Mind2Web benchmark, our best-performing model achieves a macro average element accuracy of 48.1% using GRPO that is competitive with larger models. Across training strategies, we observe that SFT yields strong baseline performance, with the language-only LoRA variant achieving 47.6% macro average—the best among SFT approaches. Interestingly, adding chain-of-thought reasoning (SFT+CoT) does not consistently improve performance, with most variants showing slight degradation compared to their SFT counterparts. However, GRPO training demonstrates clear advantages, improving the VL model from 47.2% (SFT) to 48.1%. Additionally, we observe consistency between relative categories indicating that our model generalizes well to different web domains. Similar observations can be made in the case of AndroidControl. The CoT training strategy shows mixed results on mobile tasks. For high-level control, SFT+CoT with visual-only LoRA achieves 39.0%, outperforming the best SFT approach (36.2%). However, this pattern does not hold consistently across other configurations, suggesting that the benefits of explicit reasoning may be task-dependent. The GRPO-trained GUI-Qwen (VL) achieves 44.0% accuracy on high-level tasks and 66.0% on low-level tasks, representing substantial improvements over SFT baselines. Finally, in OmniACT, all of our models cluster around 33-34% action scores, with the SFT+CoT language-only variant achieving the highest score at 34.26% with GRPO providing minimal improvements. This could be explained by the quality of the planner, as planning errors often bottleneck the overall performance [13].

#### 4.4 Analysis

**Which parameters of a non-thinking VLM can facilitate reasoning capabilities?** Recall that from the previous results (e.g. Table 1), applying LoRA adapters exclusively on the visual components of a VLM can yield performance degradation. Here, we investigate this further by comparing the performance of our model under CoT training and

<sup>2</sup><https://github.com/asweigart/pyautogui>



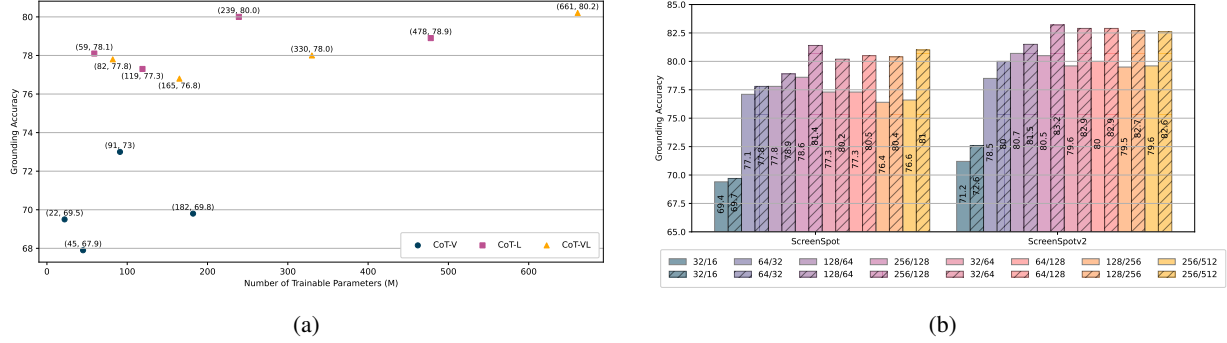


Figure 3: **(a)**: Performance of chain-of-thought models under different LoRA configurations. **(b)**: Data ablation results on ScreenSpot and ScreenSpotv2. We re-train all LoRA configurations (rank/alpha) for GUI-Qwen (VL) using the original data and the data from our filtering method. Bars with stripes (//) indicate training runs using our filtered data. Our filtering approach yields consistent improvements across all configurations.

four different LoRA adapters on the visual, language, or both backbones. Figure 3a shows the performance of these runs as a function of the number of training parameters. We observe that by controlling the total number of training parameters, injecting LoRA adapters on the language backbone yields substantial improvement compared to the visual backbone which could be attributed to differences in the expected output text distribution. This is in line with our previous findings as well as prior research in the field [44]. Finally, we observe moderate improvements in the case of vision-and-language over language-only adapters particularly for high-capacity configurations.

**What type of generations are preferred by GUI reasoning models?** In the previous experiments, we built on the assumption that the reasoning trace can guide the model’s bounding box prediction. As such, we constructed succinct traces describing the interface and/or the target element. We also observed that a model equipped with such traces enjoys benefits with regards to grounding capabilities particularly when the LoRa adapters are applied on the language backbone. However, we also observed that models trained using GRPO exhibit substantial improvement over the chain-of-thought models without imposing any strict structure on the traces. Consequently, we are interested in identifying what types of traces are preferred by these models.

For this purpose, we manually reviewed 100 randomly sampled predictions from ScreenSpot using the SFT+CoT and GRPO models. We observed that both models favoured short generations, this is expected due to the short traces present during SFT+CoT training and the reward penalizing prolonged outputs during GRPO. However, a notable distinction is that the model trained with GRPO used the tracing tokens as a “sketch pad” for the input instruction. In the vast majority of the predictions, the model tended to repeat the entire or rephrase parts of the instruction then explicitly attempt to refer to the target element (e.g. “play the next song”, <think>To play the next song, I should click on the right arrow icon.</think><answer>[445,1016,508,1053]</answer>”). This contrasts with our original hypothesis where the traces should provide a top-down summary before explicitly pointing to elements in the interface. While this behaviour still demonstrates interpretable reasoning, it reveals a more shallow reasoning pattern focused on instruction alignment rather than the deeper visual understanding we expected from chain-of-thought prompting.

**Sensitivity of RL** Despite outperforming both SFT and SFT/CoT regimes, GRPO training exhibits significant sensitivity to hyperparameters. Figure 4 illustrates the reward curves for four different LoRA configurations throughout training. While all models quickly learn to satisfy format and length constraints from the earliest training stages, we observe catastrophic model collapse in the configuration with the highest number of trainable parameters. Specifically, this configuration initially demonstrates superior performance compared to models with fewer trainable parameters during the first 250 training steps. However, after approximately 500 steps, the model collapses abruptly, yielding extremely low solution rewards. From this point until 1,000 updates, the model attempts recovery but fails to restore performance, ultimately producing zero solution rewards for the remainder of training. We hypothesise that this collapse correlates with the interplay between the number of trainable parameters and the reward function’s design. Since format and length rewards saturate early in training, the additional model capacity may be exploited to game the solution component in pursuit of total reward maximisation. This behaviour could potentially be mitigated by increasing the Kullback-Leibler (KL) penalty coefficient to constrain divergence from the base model, or rescaling the solution reward disproportionately to rewards related to the structure of the output.

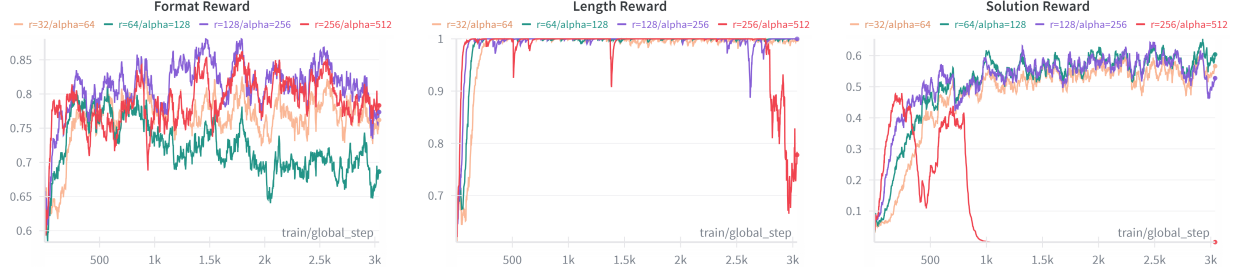


Figure 4: Reward curves for four different LoRA configurations.

**Data Ablation** To validate the effectiveness of our approach, we conduct an ablation study with GUI-Qwen (VL) using the data before and after our filtering under supervised fine-tuning. We facilitate a fair comparison under controlled conditions by applying the same training hyper-parameters and LoRA configurations. Figure 3b illustrates the performance of our model on ScreenSpot and ScreenSpotv2, when using the original data and the data produced by our filtering approach. Across all settings, we observe consistent improvements when the model is trained using our own smaller but cleaner version of the original training dataset, demonstrating the value of our data curation pipeline.

## 5 Conclusion & Limitations

In this work, we introduced an efficient training pipeline for developing reasoning-capable GUI agents by leveraging a highly curated dataset and lightweight fine-tuning strategies. Our model-based filtering framework demonstrated that high-quality, diverse, and challenging examples can be distilled from large synthetic datasets, significantly reducing data volume while improving grounding accuracy. Through systematic comparisons of supervised fine-tuning (SFT), chain-of-thought augmented SFT (SFT+CoT), and reinforcement learning with GRPO, we showed that small-scale models can match or surpass the performance of much larger baselines. Our analysis indicates that parameter-efficient adaptation via LoRA adapters plays a crucial role in eliciting reasoning behaviour, particularly when applied to the language backbone. Additionally, the filtered dataset proved critical for both data efficiency and performance stability, underscoring the importance of data quality over sheer scale in multimodal GUI reasoning. Finally, the qualitative examination of reasoning traces highlighted that current models tend to adopt shallow, instruction-alignment reasoning patterns rather than true visual abstraction, indicating promising directions for future refinement.

**Limitations** We would also like to highlight some limitations of this work that can guide future research directions. First, our filtering pipeline relies on a single model. Exploring alternative architectures, contrastive training objectives, or multi-stage ranking ensembles could improve robustness to noisy or ambiguous GUI examples. Second, while our sparse reward formulation proved effective, it remains coarse and sensitive to scaling. Future work should investigate more structured reward functions, including continuous measures of bounding-box accuracy, reasoning coherence, or multi-turn consistency. Finally, the current traces are generated and optimised for brevity. Incorporating richer reasoning rewards on the trace-level could enhance the interpretability and depth of model reasoning.

## References

- [1] Ming Li, Ruiyi Zhang, Jian Chen, Chenguang Wang, Jiuxiang Gu, Yufan Zhou, Franck Deroncourt, Wanrong Zhu, Tianyi Zhou, and Tong Sun. Towards visual text grounding of multimodal large language model. *arXiv preprint arXiv:2504.04974*, 2025.
- [2] Licheng Yu, Patrick Poirson, Shan Yang, Alexander C Berg, and Tamara L Berg. Modeling context in referring expressions. In *Computer Vision—ECCV 2016: 14th European Conference, Amsterdam, The Netherlands, October 11–14, 2016, Proceedings, Part II 14*, pages 69–85. Springer, 2016.
- [3] Bryan A Plummer, Liwei Wang, Chris M Cervantes, Juan C Caicedo, Julia Hockenmaier, and Svetlana Lazebnik. Flickr30k entities: Collecting region-to-phrase correspondences for richer image-to-sentence models. In *Proceedings of the IEEE international conference on computer vision*, pages 2641–2649, 2015.
- [4] Georgios Pantazopoulos and Eda B. Özyiğit. Towards understanding visual grounding in visual language models. *arXiv preprint arXiv:2509.10345*, 2025.

- [5] Zhiliang Peng, Wenhui Wang, Li Dong, Yaru Hao, Shaohan Huang, Shuming Ma, Qixiang Ye, and Furu Wei. Grounding multimodal large language models to the world. In *The Twelfth International Conference on Learning Representations*, 2024.
- [6] Chaoyun Zhang, He Huang, Chiming Ni, Jian Mu, Si Qin, Shilin He, Lu Wang, Fangkai Yang, Pu Zhao, Chao Du, Liqun Li, Yu Kang, Zhao Jiang, Suzhen Zheng, Rujia Wang, Jiaxu Qian, Minghua Ma, Jian-Guang Lou, Qingwei Lin, Saravan Rajmohan, and Dongmei Zhang. Ufo2: The desktop agents, 2025.
- [7] Junyang Wang, Haiyang Xu, Jiabo Ye, Ming Yan, Weizhou Shen, Ji Zhang, Fei Huang, and Jitao Sang. Mobile-agent: Autonomous multi-modal mobile device agent with visual perception. *arXiv preprint arXiv:2401.16158*, 2024.
- [8] Boyuan Zheng, Boyu Gou, Jihyung Kil, Huan Sun, and Yu Su. Gpt-4v(ision) is a generalist web agent, if grounded, 2024.
- [9] Qianhui Wu, Kanzhi Cheng, Rui Yang, Chaoyun Zhang, Jianwei Yang, Huiqiang Jiang, Jian Mu, Baolin Peng, Bo Qiao, Reuben Tan, Si Qin, Lars Liden, Qingwei Lin, Huan Zhang, Tong Zhang, Jianbing Zhang, Dongmei Zhang, and Jianfeng Gao. Gui-actor: Coordinate-free visual grounding for gui agents, 2025.
- [10] Kanzhi Cheng, Qiushi Sun, Yougang Chu, Fangzhi Xu, Li YanTao, Jianbing Zhang, and Zhiyong Wu. Seeclick: Harnessing gui grounding for advanced visual gui agents. In *Proceedings of the 62nd Annual Meeting of the Association for Computational Linguistics (Volume 1: Long Papers)*, pages 9313–9332, 2024.
- [11] Kaixin Li, Meng ziyang, Hongzhan Lin, Ziyang Luo, Yuchen Tian, Jing Ma, Zhiyong Huang, and Tat-Seng Chua. Screenspot-pro: GUI grounding for professional high-resolution computer use. In *Workshop on Reasoning and Planning for Large Language Models*, 2025.
- [12] Shravan Nayak, Xiangru Jian, Kevin Qinghong Lin, Juan A. Rodriguez, Montek Kalsi, Nicolas Chapados, M. Tamer Özsu, Aishwarya Agrawal, David Vazquez, Christopher Pal, Perouz Taslakian, Spandana Gella, and Sai Rajeswar. UI-vision: A desktop-centric GUI benchmark for visual perception and interaction. In *Forty-second International Conference on Machine Learning*, 2025.
- [13] Boyu Gou, Ruohan Wang, Boyuan Zheng, Yanan Xie, Cheng Chang, Yiheng Shu, Huan Sun, and Yu Su. Navigating the digital world as humans do: Universal visual grounding for GUI agents. In *The Thirteenth International Conference on Learning Representations*, 2025.
- [14] Yuhao Yang, Yue Wang, Dongxu Li, Ziyang Luo, Bei Chen, Chao Huang, and Junnan Li. Aria-ui: Visual grounding for gui instructions. *arXiv preprint arXiv:2412.16256*, 2024.
- [15] Kevin Qinghong Lin, Linjie Li, Difei Gao, Zhengyuan Yang, Shiwei Wu, Zechen Bai, Stan Weixian Lei, Lijuan Wang, and Mike Zheng Shou. Showui: One vision-language-action model for gui visual agent. In *Proceedings of the Computer Vision and Pattern Recognition Conference*, pages 19498–19508, 2025.
- [16] Yujia Qin, Yining Ye, Junjie Fang, Haoming Wang, Shihao Liang, Shizuo Tian, Junda Zhang, Jiahao Li, Yunxin Li, Shijue Huang, et al. Ui-tars: Pioneering automated gui interaction with native agents. *arXiv preprint arXiv:2501.12326*, 2025.
- [17] Shuyan Zhou, Frank F. Xu, Hao Zhu, Xuhui Zhou, Robert Lo, Abishek Sridhar, Xianyi Cheng, Tianyue Ou, Yonatan Bisk, Daniel Fried, Uri Alon, and Graham Neubig. Webarena: A realistic web environment for building autonomous agents. In *The Twelfth International Conference on Learning Representations*, 2024.
- [18] Izzeddin Gur, Hiroki Furuta, Austin V Huang, Mustafa Safdari, Yutaka Matsuo, Douglas Eck, and Aleksandra Faust. A real-world webagent with planning, long context understanding, and program synthesis. In *The Twelfth International Conference on Learning Representations*, 2024.
- [19] Xiang Deng, Yu Gu, Boyuan Zheng, Shijie Chen, Sam Stevens, Boshi Wang, Huan Sun, and Yu Su. Mind2web: Towards a generalist agent for the web. *Advances in Neural Information Processing Systems*, 36:28091–28114, 2023.
- [20] Run Luo, Lu Wang, Wanwei He, and Xiaobo Xia. Gui-r1: A generalist r1-style vision-language action model for gui agents. *arXiv preprint arXiv:2504.10458*, 2025.
- [21] Zhengxi Lu, Yuxiang Chai, Yaxuan Guo, Xi Yin, Liang Liu, Hao Wang, Han Xiao, Shuai Ren, Guanqing Xiong, and Hongsheng Li. Ui-r1: Enhancing efficient action prediction of gui agents by reinforcement learning. *arXiv preprint arXiv:2503.21620*, 2025.
- [22] Xinbin Yuan, Jian Zhang, Kaixin Li, Zhuoxuan Cai, Lujian Yao, Jie Chen, Enguang Wang, Qibin Hou, Jinwei Chen, Peng-Tao Jiang, et al. Enhancing visual grounding for gui agents via self-evolutionary reinforcement learning. *arXiv preprint arXiv:2505.12370*, 2025.

- [23] Daya Guo, Dejian Yang, Haowei Zhang, Junxiao Song, Ruoyu Zhang, Runxin Xu, Qihao Zhu, Shirong Ma, Peiyi Wang, Xiao Bi, et al. Deepseek-r1: Incentivizing reasoning capability in llms via reinforcement learning. *arXiv preprint arXiv:2501.12948*, 2025.
- [24] Yixin Ye, Zhen Huang, Yang Xiao, Ethan Chern, Shijie Xia, and Pengfei Liu. Limo: Less is more for reasoning. *arXiv preprint arXiv:2502.03387*, 2025.
- [25] Xuefeng Li, Haoyang Zou, and Pengfei Liu. Limr: Less is more for rl scaling. *arXiv preprint arXiv:2502.11886*, 2025.
- [26] Chaoyun Zhang, Liqun Li, Shilin He, Xu Zhang, Bo Qiao, Si Qin, Minghua Ma, Yu Kang, Qingwei Lin, Saravan Rajmohan, et al. Ufo: A ui-focused agent for windows os interaction. *arXiv preprint arXiv:2402.07939*, 2024.
- [27] Hongliang He, Wenlin Yao, Kaixin Ma, Wenhao Yu, Yong Dai, Hongming Zhang, Zhenzhong Lan, and Dong Yu. Webvoyager: Building an end-to-end web agent with large multimodal models. In *Proceedings of the 62nd Annual Meeting of the Association for Computational Linguistics (Volume 1: Long Papers)*, pages 6864–6890, 2024.
- [28] Boyuan Zheng, Boyu Gou, Jihyung Kil, Huan Sun, and Yu Su. Gpt-4v(ision) is a generalist web agent, if grounded. *arXiv preprint arXiv: 2401.01614*, 2024.
- [29] Wenyi Hong, Weihang Wang, Qingsong Lv, Jiazheng Xu, Wenmeng Yu, Junhui Ji, Yan Wang, Zihan Wang, Yuxiao Dong, Ming Ding, et al. Cogagent: A visual language model for gui agents. In *Proceedings of the IEEE/CVF Conference on Computer Vision and Pattern Recognition*, pages 14281–14290, 2024.
- [30] Peter Shaw, Mandar Joshi, James Cohan, Jonathan Berant, Panupong Pasupat, Hexiang Hu, Urvashi Khandelwal, Kenton Lee, and Kristina N Toutanova. From pixels to ui actions: Learning to follow instructions via graphical user interfaces. *Advances in Neural Information Processing Systems*, 36:34354–34370, 2023.
- [31] Zhiyong Wu, Zhenyu Wu, Fangzhi Xu, Yian Wang, Qiushi Sun, Chengyou Jia, Kanzhi Cheng, Zichen Ding, Liheng Chen, Paul Pu Liang, et al. Os-atlas: A foundation action model for generalist gui agents. *arXiv preprint arXiv:2410.23218*, 2024.
- [32] Saaket Agashe, Kyle Wong, Vincent Tu, Jiachen Yang, Ang Li, and Xin Eric Wang. Agent s2: A compositional generalist-specialist framework for computer use agents. *arXiv preprint arXiv:2504.00906*, 2025.
- [33] Rogerio Bonatti, Dan Zhao, Francesco Bonacci, Dillon Dupont, Sara Abdali, Yinheng Li, Yadong Lu, Justin Wagle, Kazuhito Koishida, Arthur Buckner, et al. Windows agent arena: Evaluating multi-modal os agents at scale. *arXiv preprint arXiv:2409.08264*, 2024.
- [34] Tianbao Xie, Danyang Zhang, Jixuan Chen, Xiaochuan Li, Siheng Zhao, Ruisheng Cao, Toh J Hua, Zhoujun Cheng, Dongchan Shin, Fangyu Lei, et al. Osworld: Benchmarking multimodal agents for open-ended tasks in real computer environments. *Advances in Neural Information Processing Systems*, 37:52040–52094, 2024.
- [35] Guanting Dong, Hongyi Yuan, Keming Lu, Chengpeng Li, Mingfeng Xue, Dayiheng Liu, Wei Wang, Zheng Yuan, Chang Zhou, and Jingren Zhou. How abilities in large language models are affected by supervised fine-tuning data composition, 2024.
- [36] Guibin Zhang, Hejia Geng, Xiaohang Yu, Zhenfei Yin, Zaibin Zhang, Zelin Tan, Heng Zhou, Zhongzhi Li, Xiangyuan Xue, Yijiang Li, Yifan Zhou, Yang Chen, Chen Zhang, Yutao Fan, Zihu Wang, Songtao Huang, Francisco Piedrahita-Velez, Yue Liao, Hongru Wang, Mengyue Yang, Heng Ji, Michael Littman, Jun Wang, Shuicheng Yan, Philip Torr, and Lei Bai. The landscape of agentic reinforcement learning for llms: A survey, 2025.
- [37] Dongyoung Kim, Sumin Park, Huiwon Jang, Jinwoo Shin, Jaehyung Kim, and Younggyo Seo. Robot-r1: Reinforcement learning for enhanced embodied reasoning in robotics. *arXiv preprint arXiv:2506.00070*, 2025.
- [38] Song Wang, Gongfan Fang, Lingdong Kong, Xiangtai Li, Jianyun Xu, Sheng Yang, Qiang Li, Jianke Zhu, and Xinchao Wang. Pixelthink: Towards efficient chain-of-pixel reasoning. *arXiv preprint arXiv:2505.23727*, 2025.
- [39] Yue Fan, Xuehai He, Diji Yang, Kaizhi Zheng, Ching-Chen Kuo, Yuting Zheng, Sravana Jyothi Narayanaraju, Xinze Guan, and Xin Eric Wang. Grit: Teaching mllms to think with images. *arXiv preprint arXiv:2505.15879*, 2025.
- [40] Yadong Lu, Jianwei Yang, Yelong Shen, and Ahmed Awadallah. Omniparser for pure vision based gui agent. *arXiv preprint arXiv:2408.00203*, 2024.
- [41] Jianwei Yang, Hao Zhang, Feng Li, Xueyan Zou, Chunyuan Li, and Jianfeng Gao. Set-of-mark prompting unleashes extraordinary visual grounding in gpt-4v. *arXiv preprint arXiv:2310.11441*, 2023.
- [42] Shuai Bai, Keqin Chen, Xuejing Liu, Jialin Wang, Wenbin Ge, Sibao Song, Kai Dang, Peng Wang, Shijie Wang, Jun Tang, et al. Qwen2. 5-vl technical report. *arXiv preprint arXiv:2502.13923*, 2025.

- [43] Edward J Hu, yelong shen, Phillip Wallis, Zeyuan Allen-Zhu, Yuanzhi Li, Shean Wang, Lu Wang, and Weizhu Chen. LoRA: Low-rank adaptation of large language models. In *International Conference on Learning Representations*, 2022.
- [44] Hugo Laurençon, Léo Tronchon, Matthieu Cord, and Victor Sanh. What matters when building vision-language models? *arXiv preprint arXiv:2405.02246*, 2024.
- [45] Zhihong Shao, Peiyi Wang, Qihao Zhu, Runxin Xu, Junxiao Song, Xiao Bi, Haowei Zhang, Mingchuan Zhang, YK Li, Y Wu, et al. Deepseekmath: Pushing the limits of mathematical reasoning in open language models. *arXiv preprint arXiv:2402.03300*, 2024.
- [46] Bavishi Rohan, Elsen Erich, Hawthorne Curtis, Nye Maxwell, Odena Augustus, Somani Arushi, and Taşlılar Sağnak. Fuyu-8b: A multimodal architecture for ai agents, October 2023.
- [47] Wei Li, William E Bishop, Alice Li, Christopher Rawles, Folawiyo Campbell-Ajala, Divya Tyamagundlu, and Oriana Riva. On the effects of data scale on ui control agents. *Advances in Neural Information Processing Systems*, 37:92130–92154, 2024.
- [48] Raghav Kapoor, Yash Parag Butala, Melisa Russak, Jing Yu Koh, Kiran Kamble, Waseem AlShikh, and Ruslan Salakhutdinov. Omniaact: A dataset and benchmark for enabling multimodal generalist autonomous agents for desktop and web. In *European Conference on Computer Vision*, pages 161–178. Springer, 2024.
- [49] Xingyu Cai, Jiayi Huang, Yuchen Bian, and Kenneth Church. Isotropy in the contextual embedding space: Clusters and manifolds. In *International Conference on Learning Representations*, 2021.

## A Data

### A.1 Filtering Pipeline

**Task Difficulty** With regards to determining challenging instances, we follow the guidelines for compute use and mobile agent from Qwen-2.5-VL<sup>3</sup>. We generate one zero-shot prediction for each training examples in the original datasets of AriaUI and ShowUI. If the center of the predicted bounding box is not within the target region, we consider this example as challenging.

**Diverse Training Examples** To select diverse training examples, given the screenshot of GUI and the instruction, we perform one forward pass from Qwen-2.5-VL 3B and obtain the last hidden state from the final layer of the model. We view this as the final representation of the multimodal sequence that captures both the image and the instruction. Following prior work [49] on clustering embeddings, we apply PCA (dim=768) on the latent representation of each example. We then apply kmeans using 10% of the initial data as centroids and select the example that is closest to each cluster. We also note that we applied clustering solely on AriaUI benchmark as it contains significantly more examples compared to ShowUI.

### A.2 Chain-of-thought traces

We extract reasoning traces in the form of explanations for each filtered instance using GPT-4o mini. Figure 5 shows the full prompt for extracting these traces. The objective of this step is to provide guidance for the fine-tuning model when deriving the solution. During extraction, we use SOM [41] to label the corresponding region and provide three in-context examples that we manually selected. We iterated over the generation prompt as during preliminary extraction we observed that the model used the prolonged generations and often referred to the SOM directly essentially providing the solution on the image.

## B Experiments

**Implementation Details** Table 6 shows the training hyperparameters for all of our models. Note that for a fair comparison, we use the same set of values for each training regime. To determine the best LoRA configuration in each experiment, we selected the model with the highest performance on ScreenSpot. Across all settings, we observed that the lower learning rate yielded the best performance in our case. Furthermore, we note that in the case of SFT with chain-of-thought, the length of the traces can vary significantly. All experiments were conducted using  $2 \times$  A100 80GB.

<sup>3</sup><https://github.com/QwenLM/Qwen3-VL/tree/main>

### Prompt for Generating Chain-of-Thought Traces

**Objective:**

Your task is to provide guidance on a visual grounding task, where given an image of a graphical user interface, and an instruction, the objective is to provide the correct bounding box that matches the instruction.

In the image that you are given there is a red ground truth bounding box and the instruction: `<instruction>`.

Below are some examples showing expected responses:

**1. Example 1:**

- Instruction: 'Close the current window'.
- Response: The image features an open Firefox browser window. To close the current window, click on 'X' icon on the top-right corner.

**2. Example 2:** For each translated question-answer pair, check for errors. For example you can identify:

- Instruction: 'Use the "Insert" button to add code'.
- Response: The image shows a LibreOffice document, the 'Insert' button is featured on the top menu next to the 'View' and 'Format' options.

**3. Example 3:**

- Instruction: 'Select Lohit Assamese font'.
- Response: The image displays a character formatting dialog in LibreOffice Writer. The 'Lohit Assamese' font is located under the family options.

You need to guide the user by an explanation that allows the user to identify the red bounding box.

**Criteria for explanation:**

- Succinct using 2 sentences at most.
- Avoid explicitly mentioning or referring to the highlighted red bounding box as the user needs to infer it directly from your explanation.
- Overall short summary of the ui.
- If the bounding box covers an element then provide a description tailored to the input instruction of the red groundtruth bounding box. If the bounding box covers plain text in the interface, refer to that text. DO NOT MENTION THAT THE BOUNDING BOX IS ALREADY HIGHLIGHTED.
- Be direct but not in the second person.

**Response format:**

You must return your response in a json format: `{"response": <response>}`, where `<response>` is your explanation.

Figure 5: Guidelines generating chain-of-thought traces.

## B.1 Ranker

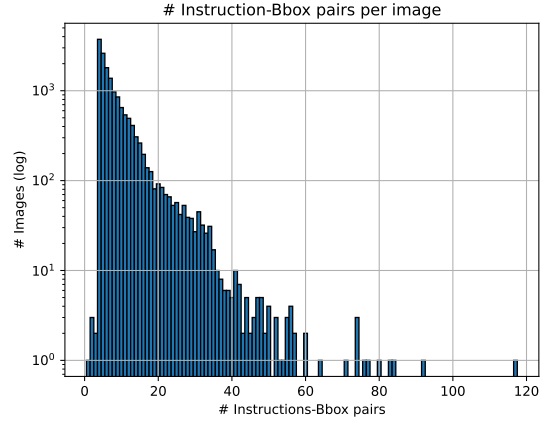
Table 8, Table 9, Table 10 illustrate the per-domain performance of our ranking model for ScreenSpot, ScreenSpotv2 and Osworld-G relative to 3B/7B/32B variants.

## B.2 Data Ablations

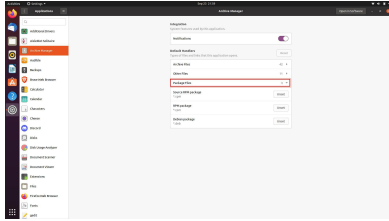
Table 11, and Table 12 illustrates detailed results regarding our data ablations. We report the grounding accuracy on ScreenSpot and Screenspotv2 with and without data filtering across all lora configurations.

Source	# Instances	# Image-Instr-Bbox Triplets
AriaUI Desktop	2668	29.3k
AriaUI Mobile	5035	52.9k
AriaUI Web	7635	45.7k
ShowUI Desktop	101	2.1k
Total	15k	130k

(a) Number of instances and positive image-instruction-bbox triplets per dataset source used to train the ranker model.

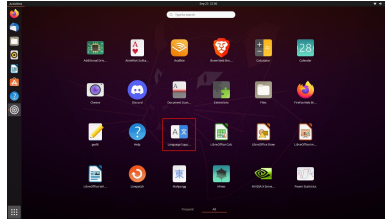


(b) Distribution of instruction-bbox pairs.



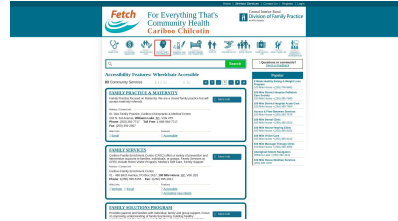
**Instruction:** Below 'Other Files' and above 'Source RPM package'.

**COT:** 'Package Files' is located between 'Other Files' and 'Source RPM package' in the 'Default Handlers' section.



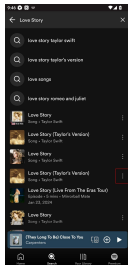
**Instruction:** Translate.

**COT:** The image shows the applications menu on a Linux desktop. The 'Language Support' app icon is relevant for the instruction 'translate'.



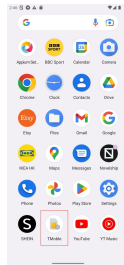
**Instruction:** Access mental health services.

**COT:** The interface includes icons for various health services. For accessing mental health services, select the icon labeled 'Mental Health & Substance Use'.



**Instruction:** Access more options for 'Love Story (Taylor's Version)'.

**COT:** The interface shows a list of search results for 'Love Story'. The three vertical dots next to 'Love Story (Taylor's Version)' provide more options for the song.



**Instruction:** Manage mobile network settings.

**COT:** The app grid includes various application icons. The 'T-Mobile' icon likely leads to mobile network settings management.



**Instruction:** Add the BRIMNES bookcase to favorites.

**COT:** The shopping cart interface lists products, including the BRIMNES bookcase. The heart-shaped icon near the bookcase represents the option to add it to favorites.

Figure 7: Examples of extracted chain-of-thought traces from desktop, web, and mobile interfaces. For clarity the correct bounding box is already drawn in the interface. Note that the instruction can target an element by describing its position, or point to an icon with underlying semantics. The goal of the trace here is to provide guidance by describing the target element or the semantics of that icon.

Hyperparameter	Ranker	SFT	SFT+CoT	GRPO
global batch size	64	{16, 32}	{16, 32}	{16, 32}
num epochs	2	{1, 2, 4}	{1, 2, 4}	{1, 2, 4}
lr	{1e-5, 5e-5}	{1e-6, 5e-6, 1e-5}	{1e-6, 5e-6, 1e-5}	{1e-6, 5e-6, 1e-5}
lr schedule	cosine decay	cosine decay	cosine decay	cosine decay
lr warmup	0.1	0.1	0.1	0.1
number of epochs	2	{1, 2, 4}	{1, 2, 4}	{1, 2, 4}
optimizer	AdamW	AdamW	AdamW	AdamW
adam betas	(0.9, 0.999)	(0.9, 0.999)	(0.9, 0.999)	(0.9, 0.999)
adam epsilon	1e-8	1e-8	1e-8	1e-8
weight decay	0.1	0.1	0.1	0.1
DeepSpeed Stage	3	3	3	3
lora modules	-	all linear layers V/L/VL	all linear layers V/L/VL	all linear layers VL
lora rank/alpha	-	{r={32, 64, 128, 256}, alpha={0.5r, 2r}}		
min pixels	3136	3136	3136	3136
max pixels	{4028160, 12845056}	846720	846720	846720
num generations	-	-	-	16
temperature	-	-	-	1
top_p	-	-	-	1.0
top_k	-	-	-	-
KL beta	-	-	-	0
reward scaling	-	-	-	1

Table 6: Hyperparameters used to train all models. For LoRA adapters V: applied on only the vision encoder and the connector, L: applied on only the language backbone, VL: applied on the entire model including the vision encoder, connector, and the language backbone.

Model	F1	Acc	Prec	Rec	F1 (Y)	F1 (N)	Prec (Y)	Prec (N)	Rec (Y)	Rec (N)
ScreenSpot										
Qwen-2.5-VL 3B*	76.2	77.6	76.1	76.3	70.5	81.9	69.7	82.5	71.3	81.4
Qwen-2.5-VL 7B*	80.3	82.3	79.1	83.1	73.9	86.6	65.4	92.8	85.0	81.2
Qwen-2.5-VL 3B Ranker	<b>93.8</b>	<b>94.2</b>	<b>93.9</b>	<b>93.8</b>	<b>92.4</b>	<b>95.3</b>	<b>92.8</b>	<b>95.0</b>	<b>92.1</b>	<b>95.5</b>
ScreenSpotv2										
Qwen-2.5-VL 3B*	78.0	78.3	78.0	78.0	75.5	80.5	75.6	80.4	75.4	80.6
Qwen-2.5-VL 7B*	82.4	83.2	81.8	84.6	78.7	86.1	70.2	93.4	89.4	79.8
Qwen-2.5-VL 3B Ranker	<b>94.5</b>	<b>94.6</b>	<b>94.5</b>	<b>94.5</b>	<b>93.8</b>	<b>95.1</b>	<b>93.5</b>	<b>95.4</b>	<b>94.2</b>	<b>94.9</b>
Osworld-G										
Qwen-2.5-VL 3B*	65.7	74.5	64.5	69.3	48.2	83.1	40.0	89.1	60.9	77.8
Qwen-2.5-VL 7B*	66.1	76.3	64.7	73.5	47.6	84.6	36.2	93.2	69.5	77.5
Qwen-2.5-VL 3B Ranker	<b>71.8</b>	<b>73.1</b>	<b>77.1</b>	<b>72.7</b>	<b>65.8</b>	<b>77.9</b>	<b>87.0</b>	<b>67.3</b>	<b>52.9</b>	<b>92.4</b>

Table 7: Performance of our ranking model on ScreenSpot, Screenspotv2 and Osworld-G benchmarks. Positive and negative classes are denoted as (Y), (N) respectively. \* denotes zero-shot evaluation.

Model	Windows		MACOS		IOS		Android		Gitlab		Shop		Forum		Tool	
	Text	Icon	Text	Icon	Text	Icon	Text	Icon	Text	Icon	Text	Icon	Text	Icon	Text	Icon
Qwen-2.5-VL 3B*	77.7	51.2	79.7	66.5	86.2	73.0	82.1	63.2	81.9	57.5	85.9	71.0	87.3	73.8	73.9	75.2
Qwen-2.5-VL 7B*	81.3	60.5	81.9	69.4	89.8	78.5	82.1	61.0	88.5	66.8	82.6	79.5	88.2	79.7	85.2	83.2
Qwen-2.5-VL 32B*	94.7	70.7	96.6	80.9	94.3	86.5	85.7	71.1	91.7	81.6	89.4	86.0	88.2	87.5	90.1	89.3
Qwen-2.5-VL 3B Ranker	96.4	80.6	98.7	86.1	98.9	93.6	96.6	89.5	97.5	82.9	97.8	93.5	93.6	92.8	89.7	93.5

Table 8: Ranking performance on ScreenSpot. \* denotes zero-shot evaluation.



Model	Windows		MACOS		IOS		Android		Gitlab		Shop		Forum		Tool	
	Text	Icon	Text	Icon	Text	Icon	Text	Icon	Text	Icon	Text	Icon	Text	Icon	Text	Icon
Qwen-2.5-VL 3B*	79.8	51.9	79.7	67.1	86.2	72.6	81.9	70.4	82.8	61.5	83.8	69.8	84.6	74.9	81.4	74.6
Qwen-2.5-VL 7B*	85.0	62.3	83.7	68.7	89.7	81.0	82.3	66.2	88.0	65.8	84.6	78.7	88.4	78.6	90.0	86.6
Qwen-2.5-VL 3B Ranker	94.9	81.7	99.5	87.1	99.1	92.2	99.3	92.6	97.0	81.4	96.6	91.4	92.3	88.7	97.5	88.4

Table 9: Ranking performance on ScreenSpotv2. \* denotes zero-shot evaluation.

Model	Text Matching	Element Recognition	Layout Understanding	Finegrained Manipulation
Qwen-2.5-VL 3B*	70.5	63.1	66.5	60.5
Qwen-2.5-VL 7B*	69.9	64.6	67.8	58.0
Qwen-2.5-VL 3B Ranker	85.2	63.9	66.8	79.0

Table 10: Ranking performance on Osvorld-G. \* denotes zero-shot evaluation.

Params (r/a)	Filtering	Windows		MACOS		IOS		Android		Gitlab		Shop		Forum		Tool		Micro Avg
		Text	Icon	Text	Icon	Text	Icon	Text	Icon	Text	Icon	Text	Icon	Text	Icon	Text	Icon	
32/16	✗	64.1	86.7	56.6	86.5	62.6	93.2	68.9	91.2	54.1	86.5	70.0	84.8	72.1	71.7	60.6	79.5	76.6
32/16	✓	70.3	91.8	61.8	94.8	70.1	98.7	68.0	92.8	62.2	92.3	76.7	88.1	67.4	82.6	65.2	79.5	81.0
64/32	✗	57.8	90.8	55.3	87.5	62.6	93.9	72.1	88.8	51.4	86.5	68.3	84.8	72.1	71.7	63.6	74.0	76.4
64/32	✓	73.4	92.9	63.2	91.7	72.0	98.0	69.7	91.2	59.5	92.3	70.0	86.4	65.1	84.8	63.6	75.3	80.4
128/64	✗	53.1	87.8	52.6	92.7	71.0	92.6	68.9	88.0	56.8	90.4	66.7	86.4	74.4	76.1	71.2	74.0	77.3
128/64	✓	68.8	91.8	63.2	92.7	70.1	98.7	68.9	95.2	56.8	92.3	76.7	88.1	69.8	80.4	60.6	75.3	80.5
256/128	✗	39.1	85.7	52.6	87.5	71.0	94.6	68.0	94.4	54.1	90.4	76.7	84.8	76.7	80.4	71.2	72.6	77.3
256/128	✓	75.0	94.9	60.5	94.8	69.2	98.7	65.6	93.6	54.1	90.4	76.7	86.4	62.8	84.8	63.6	72.6	80.2
32/64	✗	57.8	87.8	52.6	90.6	69.2	93.2	70.5	92.0	56.8	88.5	78.3	88.1	81.4	78.3	66.7	76.7	78.6
32/64	✓	71.9	93.9	64.5	92.7	73.8	98.0	66.4	92.8	67.6	94.2	78.3	89.8	69.8	82.6	59.1	78.1	81.4
64/128	✗	45.3	86.7	50.0	89.6	73.8	91.2	68.9	92.0	62.2	84.6	80.0	86.4	79.1	76.1	69.7	78.1	77.8
64/128	✓	70.3	90.8	55.3	92.7	68.2	96.0	67.2	91.2	54.1	88.5	85.0	91.5	67.4	82.6	56.1	72.6	78.9
128/256	✗	50.0	81.6	50.0	87.5	64.5	92.6	70.5	88.8	54.1	90.4	75.0	88.1	83.7	84.8	72.7	78.1	77.1
128/256	✓	62.5	89.8	51.3	94.8	63.6	93.9	68.9	92.0	46.0	94.2	78.3	89.8	60.5	82.6	63.6	74.0	77.8
256/512	✗	53.1	76.5	34.2	81.3	53.3	91.9	59.8	81.6	46.0	84.6	66.7	83.1	67.4	78.3	54.6	69.9	69.4
256/512	✓	40.6	85.7	36.8	88.5	53.3	91.9	59.8	86.4	40.5	80.8	65.0	84.8	48.8	82.6	53.0	68.5	69.7

Table 11: Grounding accuracy on ScreenSpot with and without data filtering. LoRA adapters are introduced within all linear layers of the model. Across all configurations, the data filtering approach yields greater performance (VL).

Params (r/a)	Filtering	Windows		MACOS		IOS		Android		Gitlab		Shop		Forum		Tool		Micro Avg
		Text	Icon	Text	Icon	Text	Icon	Text	Icon	Text	Icon	Text	Icon	Text	Icon	Text	Icon	
32/16	✗	66.7	87.5	68.3	91.7	70.0	93.5	73.6	92.5	58.6	90.9	63.5	88.5	71.8	77.5	59.3	80.3	79.6
32/16	✓	74.6	91.7	68.3	98.8	78.0	97.8	71.4	94.2	58.6	93.2	67.0	86.2	69.2	80.0	68.5	84.9	82.6
64/32	✗	58.7	92.7	66.7	94.1	69.0	92.8	74.7	92.5	58.6	84.1	62.6	87.7	69.2	72.5	66.7	84.9	79.5
64/32	✓	76.2	94.8	69.8	96.4	73.0	97.1	79.1	92.5	62.1	93.2	68.7	86.9	66.7	80.0	64.8	81.8	82.7
128/64	✗	58.7	89.6	57.1	97.6	76.0	94.2	75.8	92.5	69.0	88.6	60.0	88.5	74.4	77.5	66.7	78.8	80.0
128/64	✓	69.8	93.8	69.8	96.4	76.0	98.6	78.0	95.0	55.2	90.9	71.3	88.5	71.8	77.5	61.1	80.3	82.9
256/128	✗	41.3	84.4	57.1	92.9	76.0	94.9	78.0	95.8	58.6	88.6	71.3	88.5	74.4	77.5	64.8	77.3	79.6
256/128	✓	76.2	95.8	63.5	98.8	74.0	97.1	74.7	94.2	62.1	90.9	73.9	88.5	69.2	80.0	64.8	77.3	82.9
32/64	✗	58.7	89.6	58.7	95.2	71.0	93.5	78.0	93.3	69.0	88.6	68.7	87.7	79.5	77.5	59.3	83.3	80.5
32/64	✓	73.0	94.8	74.6	97.6	78.0	98.6	69.2	95.0	65.5	93.2	73.0	88.5	71.8	77.5	57.4	78.8	83.2
64/128	✗	47.6	89.6	54.0	95.2	77.0	92.0	78.0	95.0	62.1	86.4	71.3	91.5	76.9	75.0	70.4	78.8	80.7
64/128	✓	71.4	93.8	58.7	96.4	73.0	96.4	78.0	92.5	55.2	88.6	71.3	90.8	69.2	80.0	61.1	72.7	81.5
128/256	✗	49.2	82.3	55.6	92.9	67.0	92.0	74.7	91.7	62.1	86.4	67.0	86.9	79.5	85.0	74.1	78.8	78.5
128/256	✓	66.7	91.7	55.6	97.6	70.0	94.2	72.5	95.8	48.3	93.2	64.4	90.0	64.1	80.0	57.4	83.3	80.0
256/512	✗	54.0	78.1	36.5	86.9	58.0	92.0	63.7	84.2	51.7	84.1	56.5	80.8	66.7	80.0	46.3	77.3	71.2
256/512	✓	41.3	86.5	41.3	91.7	60.0	92.0	64.8	90.0	41.4	81.8	59.1	87.7	51.3	75.0	50.0	75.8	72.6

Table 12: Grounding accuracy on ScreenSpotv2 with and without data filtering. LoRA adapters are introduced within all linear layers of the model. Across all configurations, the data filtering approach yields greater performance (VL).